5-HT_{1A} Receptors Are Reduced in Temporal Lobe Epilepsy After Partial-Volume Correction

Giampiero Giovacchini, MD, PhD[1,2]; Maria T. Toczek, MD[3]; Robert Bonwetsch, MD[3]; Anto Bagic, MD[3]; Lixin Lang, PhD[1]; Charles Fraser, MS[1]; Pat Reeves-Tyer, MS[3]; Peter Herscovitch, MD[1]; William C. Eckelman, PhD[1]; Richard E. Carson, PhD[1]; and William H. Theodore, MD[3]

[1]PET Department, Clinical Center, National Institutes of Health, Bethesda, Maryland; [2]Postgraduate Specialty School in Nuclear Medicine, University of Pisa Medical School, Pisa, Italy; and [3]Clinical Epilepsy Section, National Institute of Neurological Diseases and Strokes, National Institutes of Health, Bethesda, Maryland

Preclinical studies suggest that serotonin 1A receptors (5-HT_{1A}) play a role in temporal lobe epilepsy (TLE). Previous PET studies reported decreased 5-HT_{1A} binding ipsilateral to epileptic foci but did not correct for the partial-volume effect (PVE) due to structural atrophy. **Methods:** We used PET with ^{18}F-*trans*-4-fluoro-*N*-2-[4-(2-methoxyphenyl)piperazin-1-yl]ethyl-*N*-(2-pyridyl)cyclohexanecarboxamide (^{18}F-FCWAY), a 5-HT_{1A} receptor antagonist, to study 22 patients with TLE and 10 control subjects. In patients, ^{18}F-FDG scans also were performed. An automated MR-based partial-volume correction (PVC) algorithm was applied. Psychiatric symptoms were assessed with the Beck Depression Inventory Scale. **Results:** Before PVC, significant (uncorrected $P < 0.05$) reductions of ^{18}F-FCWAY binding potential (*BP*) were detected in both mesial and lateral temporal structures, mainly ipsilateral to the seizure focus, in the insula, and in the raphe. Group differences were maximal in ipsilateral mesial temporal regions (corrected $P < 0.05$). After PVC, differences in mesial, but not lateral, temporal structures and in the insula remained highly significant (corrected $P < 0.05$). Significant (uncorrected $P < 0.05$) *BP* reductions were also detected in TLE patients with normal MR images ($n = 6$), in mesial temporal structures. After PVC, asymmetries in *BP* remained significantly greater than for glucose metabolism in hippocampus and parahippocampus. There was a significant inverse relation between the Beck Depression score and the ipsilateral hippocampal *BP*, both before and after PVC. **Conclusion:** Our study shows that in TLE patients, reductions of 5-HT_{1A} receptor binding in mesial temporal structures and insula are still significant after PVC. In contrast, partial-volume effects may be an important contributor to 5-HT_{1A} receptor-binding reductions in lateral temporal lobe. Reduction of 5-HT_{1A} receptors in the ipsilateral hippocampus may contribute to depressive symptoms in TLE patients.

Key Words: 5-HT_{1A} receptors; temporal lobe epilepsy; partial-volume correction; PET; depression

J Nucl Med 2005; 46:1128–1135

Experimental studies support a role for serotonin (5-hydroxytryptamine, 5-HT) neurotransmission in epilepsy. 5-HT_{1A} receptor activation shows antiseizure effects in partial seizure models, blocked by the highly selective 5-HT_{1A} antagonist WAY100635 (*1,2*).

In an initial PET study with ^{18}F-*trans*-4-fluoro-*N*-2-[4-(2-methoxyphenyl)piperazin-1-yl-ethyl]-*N*-(2-pyridyl)cyclohexanecarboxamide (^{18}F-FCWAY), a WAY100,635 analog (*3,4*), we reported decreased temporal 5-HT_{1A} binding ipsilateral to seizure foci in patients with temporal lobe epilepsy (TLE) (*5*). Subsequent studies using 5-HT_{1A} receptor antagonists carbonyl-^{11}C-WAY-100,635 (^{11}C-WAY) and 4,2-(methoxyphenyl)-1-[2-(*N*-2-pyridinyl)-*p*-fluorobenzamido-]ethylpiperazine (^{18}F-MPPF) reported reduced 5-HT_{1A} receptor binding in insula and anterior cingulate as well as temporal lobe (*6–8*).

However, many patients in these studies had mesial temporal sclerosis (MTS) and hippocampal atrophy on MR images. Moreover, patients with intractable TLE frequently have extrahippocampal atrophy (*9*). Owing to the partial-volume effect (PVE), brain atrophy could have affected PET findings. Thus, physiologic significance was uncertain.

To properly address this issue, MR-based partial-volume correction (PVC) is necessary (*10–12*). PVC algorithms were used in TLE studies with ^{11}C-flumazenil (*13*), and limited to mesial temporal regions, ^{18}F-FDG (*14*), and the muscarinic antagonist 4-^{123}I-iodododexetimide (*15*), but not 5-HT_{1A} ligands.

We implemented (*16*) an MR-based PVC algorithm that, for each frame, corrects gray matter activity for spill-out of gray as well as spill-in of white matter activity into gray matter pixels (*11,12*). This algorithm, appropriate for clinical investigations automatically estimated white matter activity and did not increase data variability.

In the present study we evaluated ^{18}F-FCWAY binding before and after PVC in temporal as well as extratemporal regions in a larger patient group (*5*). Patients also underwent PET with ^{18}F-FDG; PVC was applied to parametric images

Received Dec. 17, 2004; revision accepted Mar. 30, 2005.

For correspondence contact: William H. Theodore, MD, Bldg. 10, Room 5N-250, 9000 Rockville Pike, MSC 1408, National Institutes of Health, Bethesda, MD 20892-1408.

E-mail: theodorw@ninds.nih.gov

of the cerebral metabolic rate for glucose (CMRglu) as well as ^{18}F-FCWAY binding.

MATERIALS AND METHODS

Subjects

We studied 22 patients (18 men; mean age ± SD, 37 ± 11 y) referred to the Clinical Epilepsy Section, National Institute of Neurologic Disorders and Stroke (NINDS), National Institutes of Health (NIH), for evaluation of medically refractory TLE (*5*). Ictal video-electroencephalography (EEG) confirmed each patient's epileptogenic zone localization. Five had subdural recording after PET for language mapping. Epilepsy onset age was 15 ± 10 y (range, 1–34 y); disease duration was 23 ± 13 y (range, 5–46 y). Patients with structural lesions (except MTS), progressive neurologic disorders, or taking any medications aside from antiepileptic drugs (AEDs), were excluded. Eleven were included in our earlier study (*5*). None experienced seizures for at least 2 d, or a secondarily generalized tonic clonic seizure for at least 1 mo, before PET studies. Depressive symptoms were assessed with the Beck Depression Inventory (BDI) (*17*). The study was approved by the NINDS Investigational Review Board and Radiation Safety Committee. We studied 10 healthy volunteers (7 men; mean age ± SD, 35 ± 9 y), screened with general physical examination and routine laboratory tests.

MR Procedure

All subjects underwent MRI using a 1.5-T Horizon (GE Healthcare). In patients, T1-weighted spoiled gradient images (repetition time [TR], 27 ms; minimum echo time [TE]; flip angle, 20°) were acquired in coronal orientation. In healthy subjects, 3-dimensional (3D) IRprepped (variable TR; minimum TE; and inversion time, 300 ms) were acquired in the transverse plane. Coronal and transverse MR images had the same spatial resolution (voxel size, 0.94 × 0.94 × 1.5 mm; 256 × 256 × 124 slices). Transverse slices were resliced in coronal planes for analyses. Standard coronal T2 and FLAIR (Fluid Attenuated Inversion Recovery) images were obtained. All MR images were read by experienced neuroradiologists who were unaware of PET results.

Radiochemistry

^{18}F-FCWAY was synthesized as described (*3*); specific activity at injection was >18.5 TBq/mmol (>500 Ci/mmol).

PET Procedure

We used an Advance Tomograph (GE Healthcare; full width at half maximum [FWHM], 6–7 mm), scanning 35 simultaneous slices with 4.25-mm slice separation. During scanning, in a quiet, dim room with eyes closed and ears unoccluded, a thermoplastic facemask held the subject's head in place (*5*). Continuous EEG monitoring was performed to ensure interictal studies. A transmission scan was performed for attenuation correction. Subsequently, a 333 ± 74 MBq (9 ± 2 mCi) ^{18}F-FCWAY bolus was injected over 60 s and dynamic frames (1–5 min) were acquired in 3D mode for 120 min.

^{18}F-FCWAY Input Function

About 30 radial arterial samples were taken to quantify ^{18}F-FCWAY concentration and selected samples used to measure the ^{18}F-fluorocyclohexanecarboxylic acid metabolite (^{18}F-FC) (*18*). Unbound ^{18}F-FCWAY fraction plasma protein was measured with ultracentrifugation (*5*).

Data Analysis

For each subject, ^{18}F-FCWAY radioactivity frames were registered to MR images using a mutual information cost function (*16*). Tissue activity frames were corrected for brain acid metabolite ^{18}F-FC uptake, vascular radioactivity, and ^{18}F-fluoride metabolite spillover (*18*). Pixel data were fitted to a 2-tissue compartment model with 3 parameters using a metabolite-corrected input function to provide parametric images of V (*4*). A BP measurement was derived using cerebellum as a region devoid of 5-HT$_{1A}$ receptors (*19*) and calculated as:

$$BP = ([V_{ROI} - V_{CEREB}]/f_1), \quad \text{Eq. 1}$$

where V_{ROI} and V_{CEREB} are distribution volumes in the target region of interest (ROI) and cerebellum, respectively, and f_1 is the ^{18}F-FCWAY plasma free fraction. Asymmetry indices (AIs) were computed as $200\cdot(I - C)/(I + C)$, where I and C represent PET values in regions ipsilateral and contralateral to the seizure focus, respectively. In control subjects, the right side was arbitrarily called ipsilateral.

Measurement of CMRglu

Patients underwent ^{18}F-FDG PET for CMRglu measurement within 2 d of ^{18}F-FCWAY scans, using a noninvasive approach (*5*). Generated CMRglu parametric images were registered to MR images. Dosimetric restrictions precluded ^{18}F-FDG scans in control subjects.

PVC Algorithm

The algorithm (*20*) provides voxel-by-voxel binary masks of gray matter, white matter, and cerebrospinal fluid (CSF). Gray matter pixels are corrected for spill-out of gray matter activity as well as for spill-in of activity from white matter. CSF activity is set to zero. Brain white matter activity is assumed to be uniform (*11*). Visual inspection revealed poor segmentation in basal ganglia and thalamus, where a large fraction of gray pixels were misidentified as white matter, due probably to close white–gray intermixing (*16*). Since 5-HT$_{1A}$ receptor concentration in striatum and thalamus is negligible, and a 10% error in the estimation of white matter value would introduce only an ~1% error in gray matter PVC data (*11,12,16*), potential bias of ^{18}F-FCWAY binding in cortical gray regions is expected to be negligible. Subsequently, the binary masks are smoothed to the PET resolution by convolving the binary mask with a 6-mm FWHM 3D gaussian kernel (based on the reconstructed image resolution); these masks are named as s_{GM}, s_{WM}, and s_{CSF}. The corrected activity gray matter values can be calculated as follows:

$$C_{PVC} = \frac{C_{ORIG} - C_{WM}s_{WM}}{s_{GM}}, \quad \text{Eq. 2}$$

where C_{PVC} represents the corrected activity value in a gray matter pixel after PVC, C_{ORIG} is the original uncorrected pixel value, C_{WM} is the estimated white matter activity (*16*), and s_{GM} and s_{WM} are the pixel values from the smoothed masks for gray and white matter, respectively.

ROI Analysis

3D hippocampal ROIs were manually drawn on MR volumes using an anatomic atlas (*21*). Large regions ensured adequate gray matter sampling and increased signal-to-noise ratio (*16*). To minimize the risk of potential spillover of skull ^{18}F-fluoride activity, cerebellar ROIs were initially drawn along the outer cortical edge

and then uniformly shrunk by about 50%. Due to finer sampling of MR than PET data, ROIs were placed on 6 or 7 consecutive slices for amygdala, every second or third slice for hippocampus, fusiform, and parahippocampus gyrus, and every third or fourth slice for remaining cortical regions and cerebellum. A similar strategy for ROI sampling had been previously adopted in a PVC study by our group (*16*).

Raphe boundaries are best defined on PET transverse planes. Thus, PET images coregistered to (transverse and coronal) MR images were resampled to a common spatial resolution ($0.94 \times 0.94 \times 0.94$ mm) and subsequently resliced to transverse planes. Circular ROIs (about 6-mm diameter) were placed sequentially on the 13 coregistered PET slices that best visualized raphe activity. Each ROI was centered on the pixels with the highest activity. Small ROIs were chosen to minimize sensitivity to PVE.

ROI measurements were computed using only gray matter pixels, as defined by the gray matter segment (*16*). For cerebellum and raphe, where gray matter segment definition is not accurate, the mean ROI value was computed from unmasked PET images coregistered to MR volumes. Global gray matter values were calculated as cortical average values. PET measurements were not performed for thalamus and basal ganglia, where segmentation was poor. Statistical analysis was performed using *t* tests, and statistical significance set at $P < 0.05$.

RESULTS

Sixteen patients had increased hippocampal signal or mesial temporal atrophy on MR images, whereas 6 had normal MR images. Fifteen had right and 7 had left temporal ictal EEG foci. Fourteen patients had surgery; 10 are seizure-free after 1 y. The mean BDI score was 9 ± 8 (range, 0–31); 5 of 23 patients had a score of >12, the cutoff for depression (*17*).

There were no significant differences in ^{18}F-FCWAY unmetabolized or acid metabolite fraction between control subjects and patients. In controls, the ^{18}F-FCWAY fraction was 0.10 ± 0.03, 0.034 ± 0.009, and 0.021 ± 0.007, whereas the ^{18}F-FC fraction was 0.17 ± 0.04, 0.074 ± 0.020, and 0.027 ± 0.006 at 15, 60, and 120 min, respectively. The distribution volume in cerebellum (V_{CEREB}) was significantly greater in patients than that in controls (0.93 ± 0.30 vs. 0.67 ± 0.32, respectively; $P < 0.05$). The ^{18}F-FCWAY plasma free fraction (f_1) was significantly higher in patients than that in controls (0.121 ± 0.033 vs. 0.066 ± 0.024, respectively; $P < 0.001$). Cerebellar V/f_1 was significantly lower in patients than that in controls (7.9 ± 2.0 vs. 11.1 ± 5.3, respectively; $P < 0.05$). These results led us to use the form of the *BP* equation (Eq. 1) that does not divide by distribution volume in cerebellum and corrects for f_1.

Figure 1 shows coronal T2-weighted (A, top) and T1-weighed (A, bottom) MR images of a TLE patient with a right mesial temporal focus and coregistered ^{18}F-FCWAY V/f_1 (B) and CMRglu (C) images before (top) and after (bottom) PVC. Images are at the level of the posterior hippocampus, anterior to the pons. The T1- and T2-weighed images show hippocampal atrophy and dilated right ventral temporal horn, typical of MTS. Before PVC, there is clear ^{18}F-FCWAY *BP* ipsilateral mesial and lateral temporal reduction, but less CMRglu asymmetry. PVC clearly increased values in both images. However, there is no change in the pattern of asymmetric ^{18}F-FCWAY binding reduction.

In healthy subjects, *BP* values were highest in mesial temporal structures, intermediate in frontal, lateral temporal and parietal cortex, and lowest in occipital lobe (Table 1), consistent with human 5-HT$_{1A}$ receptor distribution (*19*). In patients, pre-PVC *BP* was significantly ($P < 0.05$) lower than that in control subjects in all mesial temporal regions, in ipsilateral temporal regions, and in contralateral middle temporal cortex. Reduced ^{18}F-FCWAY binding was also detected bilaterally in insula and raphe. No significant ($P < 0.05$) group differences were detected in frontal, parietal, or occipital lobes. When patients with normal MR images ($n = 6$) were compared with controls, significant *BP* reductions were detected bilaterally in parahippocampus, hippocampus, amygdala, insula, and raphe. There was no difference

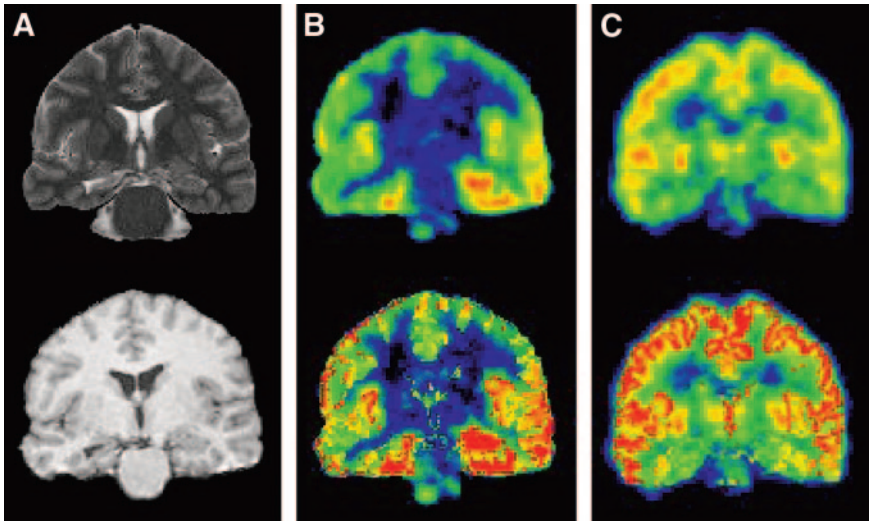

FIGURE 1. Coronal T2-weighted (A, top) and T1-weighed (A, bottom) MR images of patient with TLE with a right mesial temporal focus and coregistered ^{18}F-FCWAY distribution volume (V/f_1, B) and CMRglu (C) images before (top) and after (bottom) PVC. Coronal images are at level of posterior hippocampus, anterior to pons. V/f_1 and CMRglu images are scaled to a maximum of 100 mL/mL and 10 mg/min/100 g, respectively.

TABLE 1
BP Values (mL/mL) in Control Subjects and Patients with TLE Before and After PVC

Region	Before PVC			After PVC		
	Controls	Patients	*P*	Controls	Patients	*P*
I. Superior temporal	45 ± 15	32 ± 12	*	88 ± 25	76 ± 32	
C. Superior temporal	46 ± 13	36 ± 14		84 ± 23	73 ± 27	
I. Middle temporal	51 ± 17	37 ± 12	*	95 ± 28	79 ± 29	
C. Middle temporal	52 ± 13	41 ± 15	*	91 ± 23	77 ± 25	
I. Inferior temporal	52 ± 18	38 ± 12	*	100 ± 29	78 ± 28	
C. Inferior temporal	54 ± 16	46 ± 16		97 ± 25	90 ± 32	
I. Fusiform gyrus	73 ± 22	45 ± 15	†	126 ± 34	80 ± 24	†
C. Fusiform gyrus	71 ± 23	55 ± 19	*	120 ± 32	96 ± 32	
I. Parahippocampus	90 ± 26	47 ± 16	†	144 ± 38	83 ± 27	†
C. Parahippocampus	86 ± 23	59 ± 17	†	144 ± 41	102 ± 30	*
I. Hippocampus	88 ± 21	37 ± 17	†	127 ± 28	64 ± 31	†
C. Hippocampus	85 ± 24	58 ± 16	†	124 ± 34	97 ± 30	*
I. Amygdala	54 ± 14	33 ± 15	†	72 ± 16	50 ± 20	*
C. Amygdala	53 ± 14	42 ± 16	*	75 ± 16	60 ± 22	
I. Frontal	35 ± 11	31 ± 11		68 ± 17	66 ± 24	
C. Frontal	34 ± 10	30 ± 11		65 ± 16	63 ± 23	
I. Parietal	32 ± 10	26 ± 9		63 ± 17	64 ± 22	
C. Parietal	31 ± 10	27 ± 11		62 ± 18	66 ± 24	
I. Insula	56 ± 16	38 ± 13	†	95 ± 27	63 ± 21	†
C. Insula	55 ± 15	40 ± 14	*	95 ± 27	66 ± 21	†
I. Occipital	19 ± 6	17 ± 6		39 ± 10	44 ± 14	
C. Occipital	18 ± 4	17 ± 6		37 ± 8	46 ± 17	
Raphe	54 ± 13	38 ± 13	*	N/A	N/A	N/A

*Uncorrected $P < 0.05$, controls vs. patients, unpaired *t* test.
†$P < 0.05$ after correction for multiple region comparisons, controls vs. patients, unpaired *t* test.
I. = ipsilateral to seizure focus; C. = contralateral to seizure focus; N/A = not available.

in ^{18}F-FCWAY *BP* between patients with and without MTS in any region.

After PVC, patient–control differences remained significant in most mesial temporal regions (Table 1); in ipsilateral fusiform gyrus, parahippocampus, and hippocampus and bilaterally in the insula, group differences had a statistical significance that survived correction for multiple ROI comparisons. However, group differences were no longer significant in any lateral temporal region. No significant group differences were introduced by PVC in the frontal, parietal, and occipital cortex.

Before PVC, ^{18}F-FCWAY *BP* AIs (Table 2) were significantly ($P < 0.05$) greater in patients than those in control subjects in inferior temporal, fusiform gyrus, parahippocampus, hippocampus, amygdala, and insula. After PVC, statistical significance was lost only in the insula. Pre-PVC patient AIs were significantly greater for *BP* than for CMRglu in parahippocampus, hippocampus, and amygdala. After PVC, group differences remained significant in parahippocampus and hippocampus.

Before PVC, global gray matter *BP* was significantly ($P < 0.05$) lower in patients than that in control subjects (38 ± 11 and 54 ± 14 mL/mL, respectively). After PVC, group *BP* differences (72 ± 21 vs. 91 ± 22 mL/mL, respectively) remained significant.

In patients, global gray matter CMRglu values were 6.9 ± 1.0 mg/min/100 g before and 11.5 ± 1.9 mg/min/100 g after PVC. The estimated CMRglu white matter value was 2.39 ± 0.47 mg/min/100 g. Asymmetries between regions ipsilateral and contralateral to the epileptic focus (Table 2) were consistent with previous reports (*22,23*).

There was greater interregion variability for *BP* than for CMRglu before and after PVC. The mean percent coefficient of variation (%CV) for *BP* across ROIs (excluding raphe) was quite similar for control subjects and patients before and after PVC (controls: 28% ± 2% and 26% ± 2%, respectively; patients: 34% ± 3% and 33% ± 3%, respectively). Thus, PVC did not increase ^{18}F-FCWAY data variability. In patients, mean regional %CV for CMRglu was significantly higher ($P < 0.001$) after PVC (20% ± 2% and 17% ± 1%, respectively).

^{18}F-FCWAY *BP* and CMRglu increases after PVC varied locally, ranging in patients from about 37% to 113% for *BP* and 26% to 107% for CMRglu, respectively (Fig. 2). For *BP*, the percentage increase was lowest in amygdala, insula, and hippocampus and highest in occipital and parietal lobes. In patients, the percentage changes were significantly ($P < 0.05$) higher than those in healthy subjects bilaterally in hippocampus, frontal, parietal, and occipital lobes. The percentage increases in *BP* were significantly ($P < 0.05$ after

TABLE 2
AIs of ^{18}F-FCWAY *BP* and CMRglu Before and After PVC

Region	^{18}F-FCWAY *BP*						CMRglu			
	Before PVC			After PVC			Before PVC		After PVC	
	Controls	Patients	*P*	Controls	Patients	*P*	Patients	*P*	Patients	*P*
Superior temporal	−3 ± 8	−8 ± 12		4 ± 9	3 ± 30		−7 ± 13		1 ± 28	
Middle temporal	−5 ± 12	−7 ± 11		3 ± 8	2 ± 28		−11 ± 14		−6 ± 26	
Inferior temporal	−3 ± 13	−14 ± 13	*	2 ± 11	−12 ± 19	*	−12 ± 13		−11 ± 22	
Fusiform gyrus	3 ± 11	−17 ± 21	*	4 ± 13	−15 ± 23	*	−12 ± 14		−11 ± 20	
Parahippocampus	4 ± 5	−21 ± 16	†	1 ± 8	−20 ± 16	*	−8 ± 12	‡	−8 ± 14	§
Hippocampus	4 ± 7	−42 ± 26	†	4 ± 8	−40 ± 25	†	−14 ± 14	‡	−13 ± 16	‡
Amygdala	2 ± 15	−20 ± 20	*	−4 ± 12	−17 ± 19	*	−10 ± 14	§	−9 ± 14	
Frontal	3 ± 4	1 ± 7		4 ± 3	4 ± 15		−2 ± 3		0 ± 9	
Parietal	1 ± 5	−2 ± 13		2 ± 4	−3 ± 14		−2 ± 4		−3 ± 5	
Insula	1 ± 6	−7 ± 11	*	−1 ± 4	−5 ± 14		−6 ± 6		−5 ± 8	
Occipital	2 ± 9	−2 ± 6		2 ± 12	−2 ± 11		−2 ± 3		−2 ± 11	

*Uncorrected $P < 0.05$, controls vs. patients, unpaired *t* test.
†$P < 0.05$ after correction for multiple comparisons, controls vs. patients, unpaired *t* test.
‡$P < 0.05$ after correction for multiple region comparisons, ^{18}F-FCWAY vs. ^{18}F-FDG in patient group, paired *t* test.
§Uncorrected $P < 0.05$, ^{18}F-FCWAY vs. ^{18}F-FDG in patient group, paired *t* test.

correction for multiple ROI comparisons) greater than those in CMRglu for every region, except for occipital lobes. This finding is most likely related to the lower ratio of gray matter to white matter for ^{18}F-FCWAY than that for ^{18}F-FDG.

No significant relationship was found between CMRglu or *BP* values and either age of seizure onset or duration of epilepsy. A significant relationship (Fig. 3) was found between the BDI and ^{18}F-FCWAY *BP* but not CMRglu in ipsilateral hippocampus ($y = 47.6 - 1.24x$; $r^2 = 0.35$, $P = 0.004$), which persisted after PVC ($y = 81.2 - 1.97x$; $r^2 = 0.26$, $P = 0.016$). No significant relationships were found in other regions for both ^{18}F-FCWAY *BP* and CMRglu, before or after PVC, and BDI.

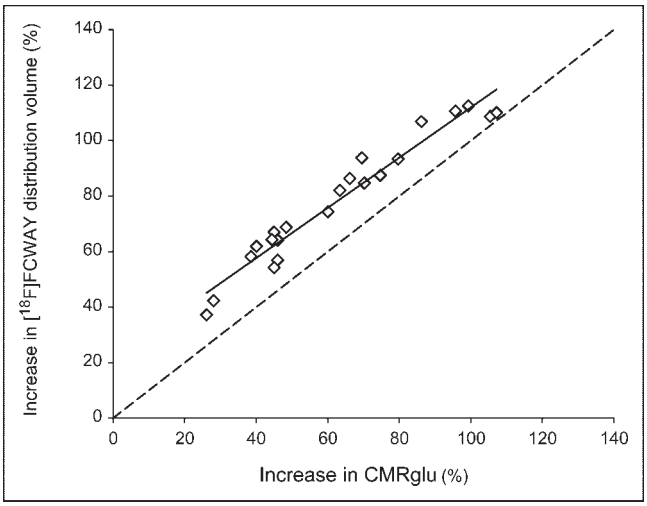

FIGURE 2. Relationship between percentage increase in ^{18}F-FCWAY distribution volume (V/f_1, mL/mL) and CMRglu (mg/min/100 g) in TLE patients. Each point represents mean ROI value. Regression equation was $V = 21.5 + 0.90$ CMRglu; $r^2 = 0.95$; $P < 0.001$. Dashed line represents identity line.

DISCUSSION

Our study shows that reduced 5-HT$_{1A}$ ^{18}F-FCWAY *BP* in mesial and insular temporal structures ipsilateral and, to a lesser extent, contralateral to temporal lobe epileptic foci is not an artifact related to PVE. Mesial temporal reductions remained significant after PVC (and correction for multiple comparisons). PVE contribution was marginal in these regions compared with the decrease in receptor binding. In contrast, reduced ^{18}F-FCWAY *BP* in lateral temporal lobe did not remain significant after PVC. No group differences were detected in frontal, parietal, and occipital lobe before or after PVC.

The finding of significant contralateral *BP* reductions is not surprising, since radiologic and histologic evidence for bilateral hippocampal pathology, and hypometabolism on PET ^{18}F-FDG studies, can be present in 30%–50% of patients with intractable TLE (*24*).

Previous 5-HT$_{1A}$ PET studies reported reduced receptor concentrations in some lateral temporal and frontal areas (*6–8*). However, in patients with TLE, atrophy is not limited to mesial structures but involves lateral temporal and frontoparietal cortex as well (*25*). In our study, these regions showed no significant differences from control in ^{18}F-FCWAY *BP* after PVC, indicating that cortical atrophy was an important contributor to reduced uncorrected values. Thus, PVE, in addition to propagation of ictal activity, might be an additional explanation for reduced 5-HT$_{1A}$ binding reported in these regions (*6*).

For both ^{18}F-FCWAY *BP* and CMRglu, there was little effect of PVC on the AIs (Table 2). This finding is likely

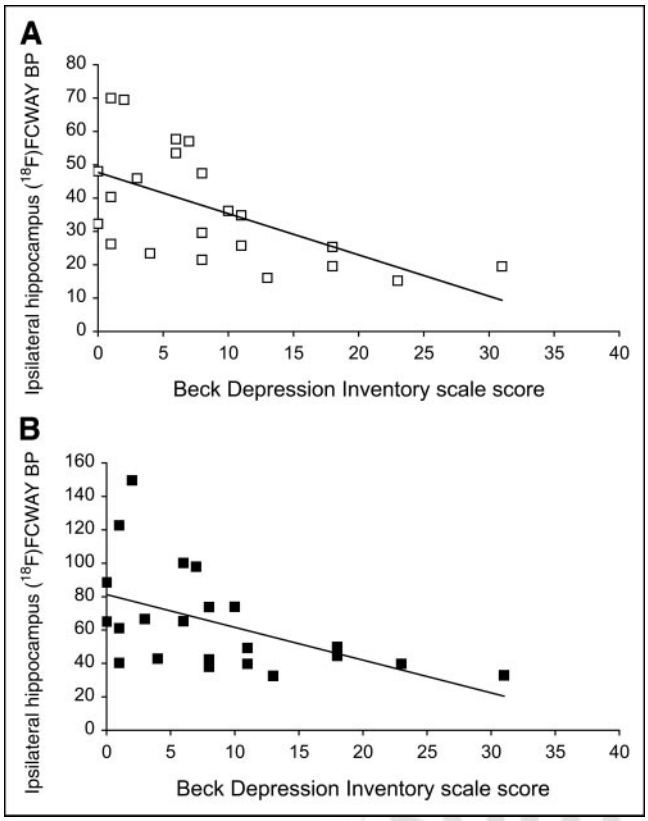

FIGURE 3. Relationship between ^{18}F-FCWAY *BP* (mL/mL) in hippocampus ipsilateral to seizure focus and BDI scale score in TLE patients before (A) and after (B) PVC. Regression equations were $y = 47.6 - 1.24x$; $r^2 = 0.35$, $P = 0.004$ (A) and $y = 81.2 - 1.97x$; $r^2 = 0.26$, $P = 0.016$ (B).

related to the fact that bilateral atrophy minimizes the magnitude of PVE. Uncorrected *BP* AIs were significantly larger than corresponding CMRglu values in hippocampus, parahippocampus, and amygdala; after PVC, statistical significance was lost only in amygdala.

PVC Algorithm

MR-based algorithms for PVC have been used successfully in PET studies of healthy aging and Alzheimer's disease (*10,11,16,26,27*). In a previous study with ^{11}C-arachidonic acid, no increase in variability after PVC was found (*16*), whereas a significant increase in variability was detected for CMRglu in the current study. For PET data with large intersubject variability, such as FCWAY *BP* and arachidonic acid incorporation rate (*16*), the additional noise of PVC is undetectable. For CMRglu, with lower intersubject variability, a moderate increase in variability owing to PVC is detectable.

Choice of Binding Index

Uncorrected V_{CEREB} was significantly greater in patients than that in control subjects. Cerebellum is assumed to be devoid of 5-HT$_{1A}$ receptors (*19*) and, thus, to provide a reliable estimate of free plus nonspecific binding (*5–8*). Since V_{CEREB} is proportional to f_1/f_2, where f_2 represents ^{18}F-FCWAY brain free fraction (*28*), this finding might be related to a combination of changes in f_1 and f_2. Subtraction of higher V_{CEREB} for regional distribution volumes (V_{ROI}, Eq. 1) might, in principle, have overestimated group differences, most likely in low binding regions—that is, occipital and parietal lobes. However, no such differences were found before or after PVC. This issue might be more relevant if a reference tissue model were adopted (*6,7*) and a different *BP* derivation used. In this case, the *BP* (*28*), is equal to:

$$Binding\ Potential = ([V_{ROI} - V_{CEREB}]/V_{CEREB}). \quad \text{Eq. 3}$$

Thus, the denominator, not just the numerator (Eq. 1), of the ratio would be affected. When this model is used, the absence of significant group differences in cerebellum binding is assumed but cannot be verified (*29,30*).

The higher value of ^{18}F-FCWAY free fraction (f_1) in patients than that in control subjects (0.121 ± 0.033 vs. 0.066 ± 0.024, respectively; $P < 0.001$) is most likely due to AED displacement of ^{18}F-FCWAY from protein-binding sites (*31*). Almost all patients were taking at least one highly protein-bound AED, such as carbamazepine, phenytoin, or valproic acid, which could have led to this effect. Correction for f_1 eliminates the bias in distribution volume measurements that would be introduced by this difference.

Increases of ^{18}F-FCWAY *BP* and CMRglu after PVC were lowest in amygdala, insula, and hippocampus and highest in occipital and parietal lobes. This finding appears to contrast with the difference between hippocampal and occipital involvement in TLE. However, regional differences in PVC effects are influenced by local geometry. Cortical gray matter pixels in thin gyri surrounded in 3 dimensions by several white matter pixels will have small s_{GM} and high s_{WM} values (Eq. 2). The opposite will occur in regions, such as hippocampus and amygdala, that are relatively homogeneous gray matter (*16*). This explains the strong linear relationship in Figure 2. The offset from the line of identity is due to a larger white matter spill-in for ^{18}F-FDG than for ^{18}F-FCWAY, since white matter *BP* is very small.

Biologic Interpretation

The *BP* used in this study (Eq. 1) is equivalent to B_{max}/K_d, where B_{max} (nmol/L/mL) is the maximum receptor concentration available for ligand binding, and K_d (nmol/L) is the ligand–receptor dissociation constant at equilibrium (*28*). Reduced *BP* may be due to decreased receptor or increased 5-HT concentration (decrease in B_{max}), decreased ligand receptor affinity (increased K_d), or a combination. Estimation of B_{max} and K_d would require at least 2 PET scans with different ^{18}F-FCWAY specific activities. This is impractical in clinical studies. Moreover, ^{18}F-FCWAY *BP* is not likely to be flow sensitive (*32*).

Previous studies in TLE patients reported greater decreases in ^{11}C-flumazenil binding than neuronal loss in mesial temporal regions ipsilateral to seizure foci (*13*).

Autoradiography performed with ^{3}H-flumazenil on surgical specimens showed reduced B_{max} and increased K_d (*13*). Preliminary results from an autoradiographic study on temporal lobectomy specimens from a subgroup of our patients indicated a decrease in B_{max}, with no changes in K_d in the hippocampus, whereas neuronal counts were diminished to a lesser extent (*33*).

Since some AEDs may increase 5-HT concentration (*5*), direct competition of the ligand with an increased 5-HT concentration cannot be excluded. However, for the serotonergic system, there is little evidence of sensitivity of high-affinity tracers, such as ^{18}F-FCWAY, to changes in 5-HT concentration (*34*). Moreover, a preliminary analysis performed on PET data did not show significant AED effects on mesial and lateral temporal or raphe ^{18}F-FCWAY *BP* values (*35*).

Our study, along with the preliminary autoradiographic results (*33*), suggests that receptor loss may be part of the initial phase of neuronal dysfunction in TLE, followed by hypometabolism and eventual structural atrophy. Since patients with new-onset epilepsy may have a low incidence of hypometabolism (*36*), ^{18}F-FCWAY PET might be particularly useful for early detection of functional abnormalities in TLE patients. Early 5-HT$_{1A}$ receptor loss might lower the seizure threshold (*1,37*). Results with both ^{11}C-flumazenil and ^{18}F-FCWAY suggest that receptor-binding studies may be of clinical value for patients with uncontrolled epilepsy being considered for surgery, particularly when other imaging studies are equivocal (*5,13*). Studies with ligands such as 5-HT$_{2A}$ receptors or the serotonin transporter, not yet performed in epilepsy patients, might be of interest as well.

The physiologic events underlying 5-HT$_{1A}$ binding reduction in raphe remain elusive. In contrast to cortex, 5-HT$_{1A}$ raphe receptors are somatodendritic. After rapid increases in extracellular 5-HT, these receptors inhibit serotonergic neuronal firing rate and, thus, 5-HT release in cortical areas (*38*). Desensitization of 5-HT$_{1A}$ autoreceptors occurs after 3–4 wk of antidepressant therapy, and a similar mechanism cannot be excluded in TLE patients (*38*).

Epilepsy and Depression

Depression is found frequently in TLE patients. In a previous study, a significant inverse correlation between the Montgomery Åsberg Depression Rating scale and ipsilateral anterior cingulate 5-HT$_{1A}$ binding was reported (*8*). We did not detect such a relationship, possibly owing to the lack of specific frontal lobe subregion sampling (*39*). However, we found a significant inverse relationship, both before and after PVC, between BDI and ^{18}F-FCWAY *BP* in hippocampus ipsilateral to the seizure focus (Fig. 3). Interestingly, no significant relationship was detected between BDI and *BP* or CMRglu in any other region. Previous PET studies in patients with depression reported reduced 5-HT$_{1A}$ receptor binding in regions relevant to epilepsy, such as raphe nuclei and the amygdala–hippocampus complex (*40*). Additional studies will be necessary to assess the relation of 5-HT$_{1A}$ receptors to depression in TLE.

CONCLUSION

Our study shows the critical importance of PVC for PET receptor studies of TLE patients refractory to medical therapy. Reduction of 5-HT$_{1A}$ *BP* remained significant in mesial, but not lateral, temporal regions of TLE patients after MR-based PVC. The decrease in 5-HT$_{1A}$ binding exceeded both CMRglu hypometabolism and hippocampal atrophy and could be detected in mesial temporal regions in patients with normal MR scans.

ACKNOWLEDGMENTS

The authors thank the entire staff of the NIH PET Department for their technical assistance. The authors thank Nicholas Patronas, MD, and John Butman, MD, for reading MR scans.

REFERENCES

1. Lu KT, Gean PW. Endogenous serotonin inhibits epileptiform activity in rat hippocampal CA1 neurons via 5-hydroxytryptamine1A receptor activation. *Neuroscience.* 1998;86:729–737.
2. Clinckers R, Smolders I, Meurs A, Ebinger G, Michotte Y. Anticonvulsant action of hippocampal dopamine and serotonin is independently mediated by D and 5-HT receptors. *J Neurochem.* 2004;89:834–843.
3. Lang L, Jagoda E, Schmall B, et al. Development of fluorine-18-labeled 5-HT$_{1A}$ antagonists. *J Med Chem.* 1999;42:1576–1586.
4. Carson RE, Lang L, Fraser C, et al. Human functional imaging with the 5-HT$_{1A}$ ligand [^{18}F]FCWAY [abstract]. *J Nucl Med.* 2002;43(suppl):55P.
5. Toczek MT, Carson RE, Lang L, et al. PET imaging of 5-HT$_{1A}$ receptor binding in patients with temporal lobe epilepsy. *Neurology.* 2003;60:749–756.
6. Merlet I, Ostrowsky K, Costes N, et al. 5-HT$_{1A}$ receptor binding and intracerebral activity in temporal lobe epilepsy: an [^{18}F]MPPF-PET study. *Brain.* 2004;127:900–913.
7. Merlet I, Ryvlin P, Costes N, et al. Statistical parametric mapping of 5-HT$_{1A}$ receptor binding in temporal lobe epilepsy with hippocampal ictal onset on intracranial EEG. *Neuroimage.* 2004;22:886–896.
8. Savic I, Lindstrom P, Gulyas B, Halldin C, Andree B, Farde L. Limbic reductions of 5-HT$_{1A}$ receptor binding in human temporal lobe epilepsy. *Neurology.* 2004;62:1343–1351.
9. Moran NF, Lemieux L, Kitchen ND, Fish DR, Shorvon SD. Extrahippocampal temporal lobe atrophy in temporal lobe epilepsy and mesial temporal sclerosis. *Brain.* 2001;124:167–175.
10. Meltzer CC, Leal JP, Mayberg HS, Wagner HN Jr, Frost JJ. Correction of PET data for partial volume effects in human cerebral cortex by MR imaging. *J Comput Assist Tomogr.* 1990;14:561–570.
11. Muller-Gartner HW, Links JM, Prince JL, et al. Measurement of radiotracer concentration in brain gray matter using positron emission tomography: MRI-based correction for partial volume effects. *J Cereb Blood Flow Metab.* 1992;12:571–583.
12. Meltzer CC, Kinahan PE, Greer PJ, et al. Comparative evaluation of MR-based partial-volume correction schemes for PET. *J Nucl Med.* 1999;40:2053–2065.
13. Koepp MJ, Hand KS, Labbe C, et al. In vivo [^{11}C]flumazenil-PET correlates with ex vivo [^{3}H]flumazenil autoradiography in hippocampal sclerosis. *Ann Neurol.* 1998;43:618–626.
14. Knowlton RC, Laxer KD, Klein G, et al. In vivo hippocampal glucose metabolism in mesial temporal lobe epilepsy. *Neurology.* 2001;57:1184–1190.
15. Weckesser M, Hufnagel A, Ziemons K, et al. Effect of partial volume correction on muscarinic cholinergic receptor imaging with single-photon emission tomography in patients with temporal lobe epilepsy. *Eur J Nucl Med.* 1997;24:1156–1161.
16. Giovacchini G, Lerner A, Toczek MT, et al. Brain incorporation of [^{11}C]arachidonic acid, blood volume, and blood flow in healthy aging: a study with partial-volume correction. *J Nucl Med.* 2004;45:1471–1479.
17. Beck AT, Steer RA, Ball R, Ranieri W. Comparison of Beck Depression

Inventories-IA and -II in psychiatric outpatients. *J Pers Assess.* 1996;67:588–597.
18. Carson RE, Wu Y, Lang L, et al. Brain uptake of the acid metabolites of [^{18}F]-labeled WAY 100635 analogs. *J Cereb Blood Flow Metab.* 2003;23:249–260.
19. Hall H, Lundkvist C, Halldin C, et al. Autoradiographic localization of 5-HT$_{1A}$ receptors in the post-mortem human brain using [^{3}H]WAY-100635 and [^{11}C]WAY-100635. *Brain Res.* 1997;745:96–108.
20. Pham DL, Prince JL. Adaptive fuzzy segmentation of magnetic resonance images. *IEEE Trans Med Imaging.* 1999;18:737–752.
21. Duvernoy HM. *The Human Hippocampus: Functional Anatomy, Vascularization and Serial Sections with MRI.* 2nd ed. Berlin, Germany: Springer; 1998.
22. Henry TR, Mazziotta JC, Engel J Jr, et al. Quantifying interictal metabolic activity in human temporal lobe epilepsy. *J Cereb Blood Flow Metab.* 1990;10:748–757.
23. Kim YK, Lee DS, Lee SK, et al. Differential features of metabolic abnormalities between medial and lateral temporal lobe epilepsy: quantitative analysis of [^{18}F]FDG PET using SPM. *J Nucl Med.* 2003;44:1006–1012.
24. Van Paesschen W, Sisodiya S, Connelly A, et al. Quantitative hippocampal MRI and intractable temporal lobe epilepsy. *Neurology.* 1995;45:2233–2240.
25. Marsh L, Morrell MJ, Shear PK, et al. Cortical and hippocampal volume deficits in temporal lobe epilepsy. *Epilepsia.* 1997;38:576–587.
26. Ibanez V, Pietrini P, Alexander GE, et al. Regional glucose metabolic abnormalities are not the result of atrophy in Alzheimer's disease. *Neurology.* 1998;50:1585–1593.
27. Meltzer CC, Cantwell MN, Greer PJ, et al. Does cerebral blood flow decline in healthy aging? A PET study with partial-volume correction. *J Nucl Med.* 2000;41:1842–1848.
28. Mintun MA, Raichle ME, Kilbourn MR, Wooten GF, Welch MJ. A quantitative model for the in vivo assessment of drug binding sites with positron emission tomography. *Ann Neurol.* 1984;15:217–227.
29. Lammertsma AA, Hume SP. Simplified reference tissue model for PET receptor studies. *Neuroimage.* 1996;4:153–158.
30. Gunn RN, Lammertsma AA, Hume SP, Cunningham VJ. Parametric imaging of ligand-receptor binding in PET using a simplified reference region model. *Neuroimage.* 1997;6:279–287.
31. Surks MI, DeFesi CR. Normal serum free thyroid hormone concentrations in patients treated with phenytoin or carbamazepine: a paradox resolved. *JAMA.* 1996;275:1495–1498.
32. Carson RE, Lang L, Watabe H, et al. PET evaluation of [^{18}F]FCWAY, an analog of the 5-HT$_{1A}$ receptor antagonist, WAY-100635. *Nucl Med Biol.* 2000;27:493–497.
33. Jagoda EM, Gillespie TF, Lang L, et al. Decrease in 5HT$_{1A}$ receptor density corresponds to neural losses in the hippocampus of epileptic patients but not in the cortex of the temporal lobe [abstract]. *J Nucl Med.* 2004;45(suppl):14P.
34. Giovacchini G, Lang L, Ma Y, Herscovitch P, Eckelman WC, Carson RE. Differential effects of the selective serotonin reuptake inhibitor paroxetine on raphe and cortical 5-HT$_{1A}$ binding: a PET study in monkeys with [^{18}F]FPWAY [abstract]. *J Nucl Med.* 2004;45(suppl):8P.
35. Theodore WH, Giovacchini G, Toczek M, et al. The effect of carbamazepine on PET 5-HT$_{1A}$ ligand binding in patients with temporal lobe epilepsy [abstract]. *Neuroimage.* 2004;22:P163.
36. Gaillard WD, Kopylev L, Weinstein S, et al. Low incidence of abnormal [^{18}]FDG-PET in children with new-onset partial epilepsy: a prospective study. *Neurology.* 2002;58:717–722.
37. Sarnyai Z, Sibille EL, Pavlides C, Fenster RJ, McEwen BS, Toth M. Impaired hippocampal-dependent learning and functional abnormalities in the hippocampus in mice lacking serotonin$_{1A}$ receptors. *Proc Natl Acad Sci USA.* 2000;97:14731–14736.
38. Blier P, Ward NM. Is there a role for 5-HT$_{1A}$ agonists in the treatment of depression? *Biol Psychiatry.* 2003;53:193–203.
39. Drevets WC, Price JL, Simpson JR Jr, et al. Subgenual prefrontal cortex abnormalities in mood disorders. *Nature.* 1997;386:824–827.
40. Drevets WC, Frank E, Price JC, et al. PET imaging of serotonin 1A receptor binding in depression. *Biol Psychiatry.* 1999;46:1375–1387.

JNM The Journal of NUCLEAR MEDICINE

5-HT$_{1A}$ Receptors Are Reduced in Temporal Lobe Epilepsy After Partial-Volume Correction

Giampiero Giovacchini, Maria T. Toczek, Robert Bonwetsch, Anto Bagic, Lixin Lang, Charles Fraser, Pat Reeves-Tyer, Peter Herscovitch, William C. Eckelman, Richard E. Carson and William H. Theodore

J Nucl Med. 2005;46:1128-1135.

The Journal of Nuclear Medicine is published monthly.
SNMMI | Society of Nuclear Medicine and Molecular Imaging
1850 Samuel Morse Drive, Reston, VA 20190.
(Print ISSN: 0161-5505, Online ISSN: 2159-662X)

SNMMI SOCIETY OF NUCLEAR MEDICINE AND MOLECULAR IMAGING